FOCUS ISSUE OF SELECTED PRESENTATIONS FROM IMLB 2014

High-Performance Lithium-Ion Polymer Cells Assembled with Composite Polymer Electrolytes based on Core-Shell Structured SiO_2 Particles Containing Poly(lithium acrylate) in the Shell

Se-Mi Park, Yoon-Sung Lee, and Dong-Won Kim*,z

Department of Chemical Engineering, Hanyang University, Seungdong-gu, Seoul 133-791, Korea

Core-shell structured SiO_2 nanoparticles containing poly(lithium acrylate) in the shell were synthesized and used as functional fillers in composite polymer electrolytes for lithium-ion polymer cells. The composite polymer electrolytes prepared with $SiO_2(Li^+)$ particles exhibited high ionic conductivity, good thermal stability, and favorable interfacial characteristics. By using these composite polymer electrolytes, lithium-ion polymer cells composed of a graphite negative electrode and a $LiNi_{0.6}Co_{0.2}Mn_{0.2}O_2$ positive electrode were assembled, and their cycling performance was evaluated. The cells assembled with composite polymer electrolytes containing a proper amount of $SiO_2(Li^+)$ particles exhibited good cycling performance at both at ambient and elevated temperatures.
 [DOI: 10.1149/2.0081502jes]

Manuscript submitted September 30, 2014; revised manuscript received December 9, 2014. Published December 31, 2014. This was Paper 676 presented at the Como, Italy, Meeting of the IMLB, June 10–14, 2014. *This paper is part of the Focus Issue of Selected Presentations from IMLB 2014.*

Lithium-ion polymer cells which employ polymer electrolytes have been widely investigated for applications in portable electronic devices, electric vehicles, and energy storage systems.[1–4] Although the ionic conductivities of gel polymer electrolytes usually exceed 10^{-3} S cm^{-1} at ambient temperature, the host polymers usually lose their mechanical strength when they are plasticized by organic solvents. Thus, porous polyolefin separators are now being used to provide mechanical support in commercialized lithium-ion polymer batteries. In order to obtain gel polymer electrolytes with enhanced mechanical strength, inert inorganic fillers such as SiO_2, Al_2O_3, TiO_2, and $BaTiO_3$ have been incorporated into the gel polymer electrolytes.[5–14] In these composite polymer electrolytes, the inorganic particles improve the mechanical properties of the gel polymer electrolytes through physical action without directly contributing to the lithium-ion transport process. In our previous studies, core-shell structured SiO_2 particles containing poly(lithium 4-styrene sulfonate) in the shell were synthesized and used in preparing Li^+-conducting composite polymer electrolytes.[15–18] In this study, we synthesized core-shell-structured SiO_2 particles containing poly(lithium acrylate) in the shell, because poly(lithium acrylate) is expected to be more compatible with carbonate-based liquid electrolytes such as ethylene carbonate (EC) and diethylene carbonate (DEC). Unlike conventional ceramic fillers, the core-shell-structured SiO_2 particles containing poly(lithium acrylate) act as a source of Li^+ ions in the composite polymer electrolyte, because mobile Li^+ ions dissociate out of the shell of the particles. The $SiO_2(Li^+)$ nanoparticles were incorporated into a poly(vinylidene fluoride-*co*-hexafluoropropylene) (P(VdF-co-HFP)) matrix polymer to make a thin porous composite polymer membrane, and the membrane was activated by soaking with liquid electrolyte to form the composite polymer electrolyte. The effect of the amount of core-shell $SiO_2(Li^+)$ particles was investigated in detail in order to provide the composite polymer electrolyte with high ionic conductivity, good thermal stability, and favorable interfacial characteristics. The composite polymer electrolyte was utilized in a lithium-ion polymer cell composed of a graphite negative electrode and a $LiNi_{0.6}Co_{0.2}Mn_{0.2}O_2$ positive electrode. The cycling performance of the cells was evaluated and compared to that of cells assembled with liquid electrolyte.

Experimental

Synthesis of core-shell structured $SiO_2(Li^+)$ particles.— Figure 1 illustrates the synthetic scheme of core-shell structured SiO_2 nanoparticles containing poly(lithium acrylate) in the shell. Vinyltrimethoxysilane (VTMS, Evonik) was added to double distilled water while stirring until the VTMS droplets completely disappeared. A catalytic amount of ammonium hydroxide solution (28 wt%, Junsei) was then added to the solution, and the reaction was continued for 12 h at ambient temperature. After completion of the reaction, the resulting precipitate (silica core particles with vinyl groups) was centrifuged and washed several times with ethanol. The core-shell-structured $SiO_2(Na^+)$ particles were synthesized by radical copolymerization of silica core particles and sodium acrylate (Sigma-Aldrich) with ammonium persulfate (Sigma-Aldrich) in distilled water at 85°C for 48 h. After polymerization, the precipitate was filtered and the Na^+ ions in poly(sodium acrylate) of the shell were replaced with Li^+ ions by ionic exchange with $LiOH \cdot H_2O$.

Preparation of composite polymer electrolytes.— A composite polymer film consisting of P(VdF-*co*-HFP)(Kynar 2801, Mw = 380,000) and core-shell-structured $SiO_2(Li^+)$ nanoparticles was prepared by mixing P(VdF-*co*-HFP), $SiO_2(Li^+)$ particles and dibutyl phthalate (DBP) in acetone by ballmilling, and subsequent casting using a doctor blade. The resulting film was immersed in methanol for pore formation by removing DBP, and the film was then vacuum dried at 70°C for 12 h. The content of core-shell $SiO_2(Li^+)$ nanoparticles in the composite polymer membrane varied from 0 to 8.0 wt%. The thickness of the composite polymer membrane was kept at 25 μm in order to compare their physical properties with those of the polypropylene separator (Celgard 2400, 25 μm). Free-standing composite polymer electrolyte films were finally obtained by soaking the membranes in 1.15 M $LiPF_6$-EC/DEC (3:7 by volume) containing 1.0 wt% vinylene carbonate (VC) (battery grade, Soulbrain Co.).

Electrode preparation and cell assembly.— The $LiNi_{0.6}Co_{0.2}Mn_{0.2}O_2$ electrode was prepared by coating a N-methyl pyrrolidone (NMP)-based slurry containing $LiNi_{0.6}Co_{0.2}Mn_{0.2}O_2$ powder, poly(vinylidene fluoride) (PVdF), and super-P carbon (MMM Co.) (85:7.5:7.5 by weight) onto an Al foil. The carbon electrode was similarly prepared by coating an NMP-based slurry of mesocarbon microbeads (MCMB, Osaka Gas), PVdF, and super-P carbon (88:8:4 by weight) onto a Cu foil. A lithium-ion polymer cell composed

*Electrochemical Society Active Member.
zE-mail: dongwonkim@hanyang.ac.kr

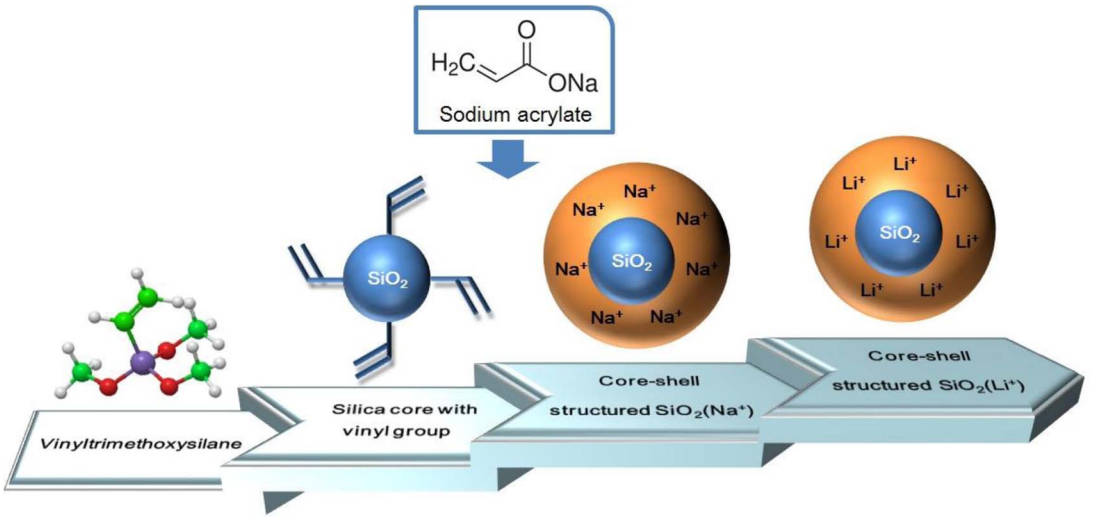

Figure 1. Reaction scheme for synthesis of core-shell-structured $SiO_2(Li^+)$ particles containing poly(lithium acrylate) in the shell.

of a single stack was assembled by sandwiching the composite polymer electrolyte between the graphite negative electrode and the $LiNi_{0.6}Co_{0.2}Mn_{0.2}O_2$ positive electrode. Other than the composite polymer electrolyte, no additional liquid electrolyte was added to the cell. For comparison, a liquid electrolyte-based lithium-ion cell was also assembled with a polypropylene separator (Celgard 2400) and the same liquid electrolyte (1.15 M $LiPF_6$-EC/DEC + 1 wt% VC). The cell was enclosed in a metalized plastic pouch and was vacuum sealed in a glove box filled with argon gas. The electrolyte loss was negligible during vacuum sealing of the cells.

Characterization and measurements.— The morphology of the silica core particles was examined using a field-emission scanning electron microscope (FE-SEM, JEOL JSM-6330F). Fourier transform infrared (FT-IR) spectra were recorded on a Magna IR 760 spectrometer in the range of 400–4000 cm^{-1} with KBr powder-pressed pellets. The core-shell structured SiO_2 particles were characterized by a field-emission transmission electron microscope (FE-TEM, FEI JEM 2100F) equipped with energy dispersive X-ray spectroscopy (EDXS) for line scanning analysis. The thermal shrinkage of the composite polymer membranes was measured in terms of their dimensional changes after being held at 140°C for 30 min. AC impedance measurements were performed to measure ionic conductivity and interfacial resistance using a Zahner Electrik IM6 impedance analyzer over a frequency range of 100 kHz to 1 mHz with an amplitude of 10 mV. Charge and discharge cycling tests of the lithium-ion polymer cells were conducted at a current of 0.5 C rate over a voltage range of 2.6 to 4.3 V using battery testing equipment (WBCS 3000, Wonatech) at room temperature. HF content in the electrolyte was measured by a neutralization titration method after the cell was stored in a 55°C oven for 3 days.[19] Methyl orange was used as an acid-base indicator.

Results and Discussion

Figure 2a shows the FE-SEM image of silica core particles. The SiO_2 particles have uniform spherical shapes with an average diameter of 260 nm. From the FT-IR spectrum of the silica particles shown in Fig. 2b, symmetric stretching vibrations of the siloxane (Si-O-Si) group appeared at 766 cm^{-1}, while asymmetric stretching vibrations of siloxane were observed between 1000 and 1200 cm^{-1}. The spectrum also revealed two sharp peaks at 1410 and 1603 cm^{-1}, which correspond to the characteristic peaks of the C=C double bond,[20–22] indicating that the silica particles contain vinyl groups. These reactive vinyl groups permit the growth of silica particles by radical polymerization with sodium acrylate to produce core-shell structured silica particles.

Figure 3a shows a TEM image of a core-shell structured silica nanoparticle containing poly(sodium acrylate) in the shell. The

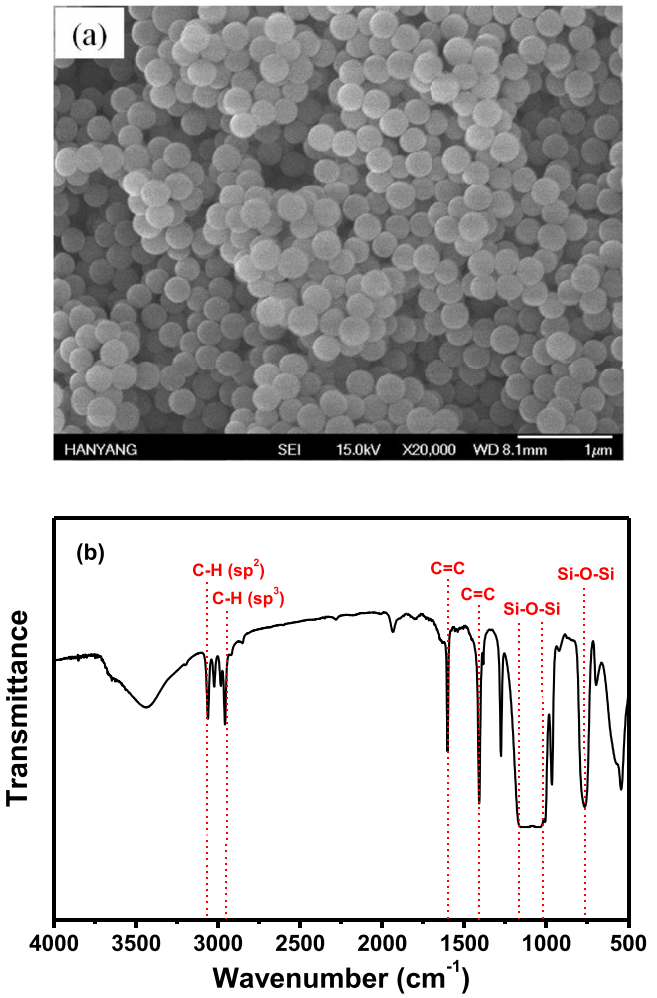

Figure 2. (a) FE-SEM image and (b) FT-IR spectrum of SiO_2 nanoparticles with vinyl groups.

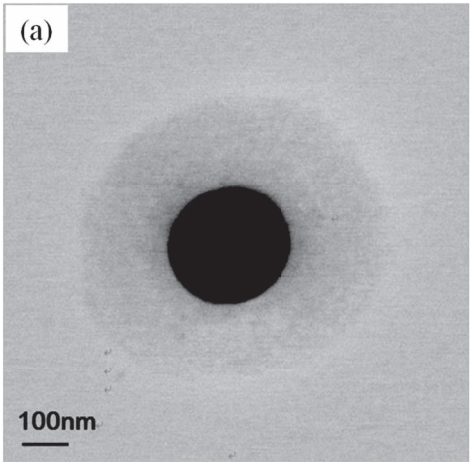

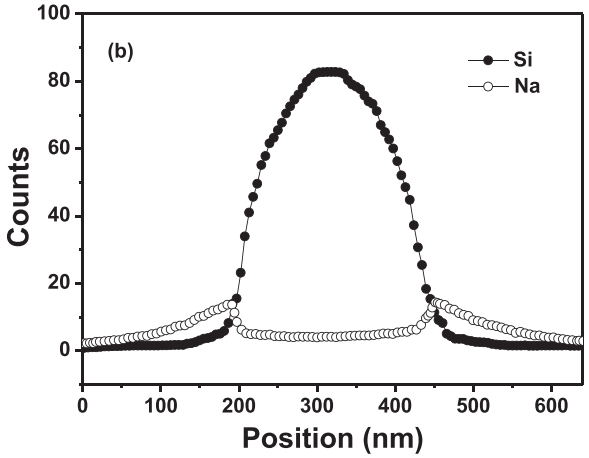

Figure 3. (a) TEM image and (b) EDXS profile of a core-shell-structured $SiO_2(Na^+)$ nanoparticle.

particle has a uniform core-shell morphology with a 190 nm thick shell layer of poly(sodium acrylate) surrounding a SiO_2 core particle. The SiO_2 core diameter was estimated to be about 260 nm, which is consistent with the image shown in Fig. 2a. An EDXS profile in the direction of the diameter of the core-shell SiO_2 particle (Fig. 3b) reveals that the silicon atoms are positioned at the particle core (∼260 nm), while sodium atoms arising from the poly(sodium acrylate) appear in the shell (∼190 nm). This result is well consistent with the TEM image shown in Fig. 3a, confirming that the SiO_2 particle was encapsulated by poly(sodium acrylate) with a uniform thickness and that spherical core-shell-structured SiO_2 particles were successfully synthesized. Using these core-shell-structured SiO_2 particles, we replaced the sodium ions in poly(sodium acrylate) with lithium ions by ion exchange. The XPS spectrum of the resulting core-shell-structured SiO_2 particles revealed a 57.4 eV characteristic peak corresponding to lithium,[23] indicating that the $SiO_2(Na^+)$ particles were converted to $SiO_2(Li^+)$ particles.

The addition of $SiO_2(Li^+)$ nanoparticles provided sufficient mechanical integrity to make a freestanding membrane with a thickness of 25 μm. From the energy dispersive X-ray spectroscopy analysis, the $SiO_2(Li^+)$ nanoparticles were observed to be homogeneously distributed in the composite polymer membrane without agglomeration. Composite polymer electrolyte was obtained by soaking the membrane in liquid electrolyte. The electrolyte solution was well encapsulated in the composite polymer membrane because the carboxylate group in the shell was highly compatible with the carbonate-based electrolyte, which allowed suppression of solvent exudation from the composite polymer electrolyte. Figure 4 shows the ionic conductivity of composite polymer electrolytes as a function of the $SiO_2(Li^+)$ content. The ionic conductivity increases with increasing $SiO_2(Li^+)$ content, up to a maximum at 4.0 wt%, and decreases with further increase in $SiO_2(Li^+)$ content. The initial increase in ionic conductivity is associated with the enhancement of electrolyte uptake as well as the increase in mobile lithium ions dissociating out from poly(lithium acrylate) in the shell of the SiO_2 particles. The generation of free volume with the addition of $SiO_2(Li^+)$ nanoparticles may also contribute to the improved ionic conductivity, as previously reported in other composite polymer electrolyte systems.[7] The decrease in ionic conductivity beyond 4.0 wt% $SiO_2(Li^+)$ can be ascribed to the blocking effect of the charge carrier transport, as the SiO_2 core of the $SiO_2(Li^+)$ powder is an insulator by nature. Ionic conductivity of the composite polymer electrolyte prepared with 4.0 wt% $SiO_2(Li^+)$ was 1.8×10^{-3} S cm^{-1} at room temperature.

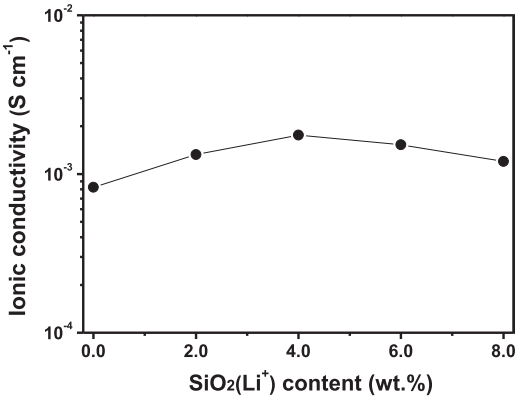

Figure 4. Ionic conductivities of the composite polymer electrolytes containing different contents of core-shell-structured $SiO_2(Li^+)$ nanoparticles.

In order to evaluate the heat resistance of the composite polymer membranes containing $SiO_2(Li^+)$ nanoparticles, we measured the thermal shrinkage after storing them at 140°C for 30 min, and the results are given in Fig. 5. For comparison, the PP separator was also exposed to the same thermal conditions. As shown in Fig. 5a, the PP separator exhibited a high degree of shrinkage (31.2%) during exposure to the high temperature conditions. Because the manufacturing process of microporous PP separator includes stretching processes, the PP separator easily shrinks when exposed to high temperature, which may result in a short circuit between negative electrode and positive electrode. In contrast, the composite polymer membranes showed little change in their dimension. As the content of $SiO_2(Li^+)$ particles increased, the membrane turned into a white opaque film, and its mechanical strength was improved. This indicates that the incorporation of $SiO_2(Li^+)$ particles resulted in a filler network providing mechanical integrity and thermal stability to the composite membrane.

Composite polymer electrolytes containing $SiO_2(Li^+)$ nanoparticles were used to assemble lithium-ion polymer cells composed of a graphite negative electrode and a $LiNi_{0.6}Co_{0.2}Mn_{0.2}O_2$ positive electrode. Figure 6a shows the typical charge-discharge curves of the

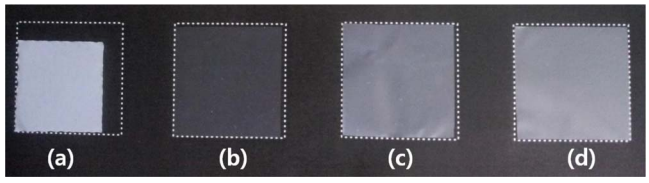

Figure 5. Photographs of a PP separator and composite polymer membranes containing different contents of $SiO_2(Li^+)$ nanoparticles after being held at 140°C for 30 min. (a) PP separator, (b) polymer membrane without $SiO_2(Li^+)$, (c) composite polymer membrane containing 4 wt% $SiO_2(Li^+)$ and (d) composite polymer membrane containing 8 wt% $SiO_2(Li^+)$.

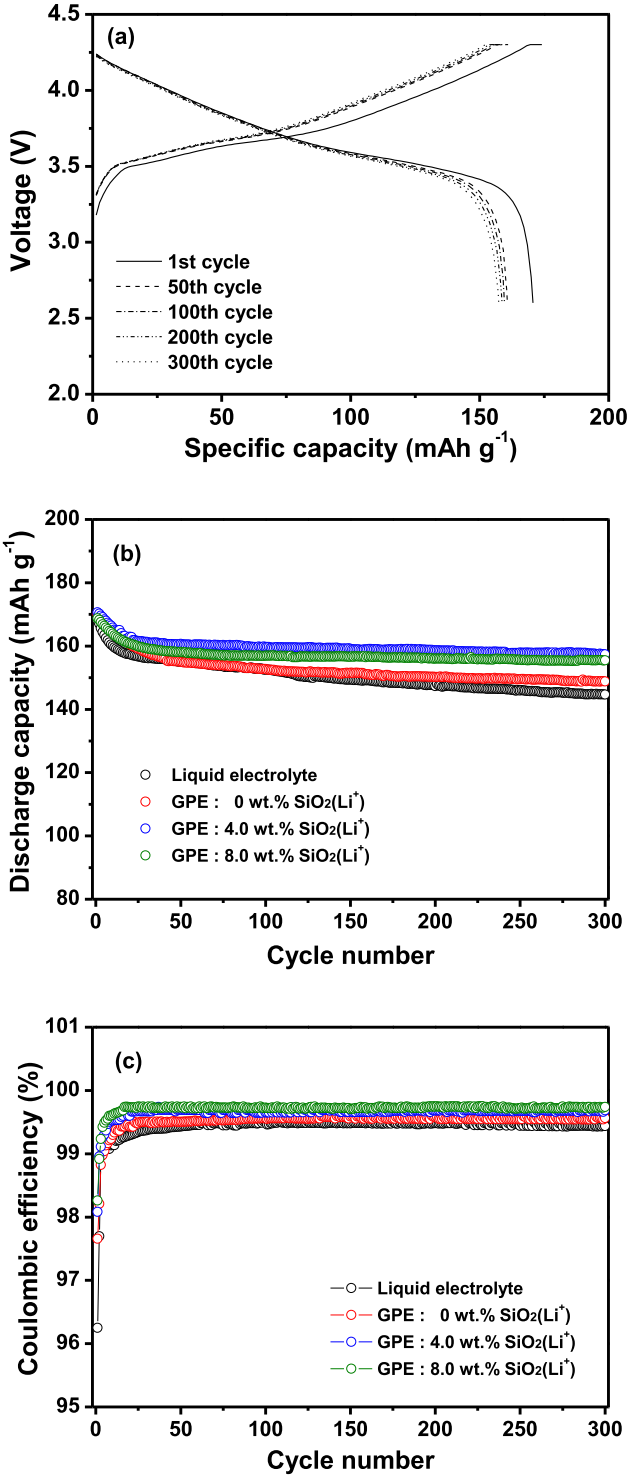

Figure 6. (a) Charge and discharge curves of the lithium-ion polymer cell assembled with composite polymer electrolyte containing 4 wt% $SiO_2(Li^+)$ nanoparticles at 25°C (0.5 C CC and CV charge, 0.5 C CC discharge, cut-off: 2.6–4.3 V), (b) discharge capacities of the lithium-ion polymer cells assembled with different electrolytes, and (c) coulombic efficiencies of the lithium-ion polymer cells assembled with different electrolytes.

1st, 50th, 100th, 200th, and 300th cycle of the lithium-ion polymer cell assembled with the composite polymer electrolyte containing 4.0 wt% $SiO_2(Li^+)$ particles. The cell delivered an initial discharge capacity of 170.7 mAh g^{-1} based on the active $LiNi_{0.6}Co_{0.2}Mn_{0.2}O_2$ material in the positive electrode. Note that the capacity recovered during constant voltage charging was very small, which suggests that the cell has a very low internal cell resistance and is thus capable of delivering high capacity. The cell exhibited very stable cycling characteristics; that is, it delivered 92.2% of the initial discharge capacity after 300 cycles. Figure 6b shows the discharge capacity versus cycle number of lithium-ion polymer cells assembled with composite polymer electrolytes containing different amounts of $SiO_2(Li^+)$ particles. For comparison, the cycling results of the cells assembled with liquid electrolyte using a PP separator or polymer electrolyte without $SiO_2(Li^+)$ particles are also given in Fig. 6b. The initial discharge capacity slightly increased with the addition of $SiO_2(Li^+)$ particles up to 4.0 wt%, which is in accordance with the increase in ionic conductivity, as shown in Fig. 4. Capacity retention was improved by increasing the $SiO_2(Li^+)$ content in the composite polymer electrolyte. Poly(lithium acrylate) in the shell of the $SiO_2(Li^+)$ particles has a carboxylate group to effectively hold the organic solvent. Thus, the ability to retain the electrolyte solution in the composite polymer membrane was provided by the addition of $SiO_2(Li^+)$ particles, which help prevent exudation of the electrolyte solution during cycling. The stable interfacial characteristics promoted by the $SiO_2(Li^+)$ powder may also contribute to the improved capacity retention.[5–7,24] Coulombic efficiencies of the cells with $SiO_2(Li^+)$ particles were higher than those of the liquid electrolyte-based cell through cycling, as shown in Fig. 6c. The coulombic efficiency slightly increased with increasing content of $SiO_2(Li^+)$ particles in the composite polymer electrolytes, indicating that the use of the core-shell structured SiO_2 particles containing poly(lithium acrylate) can improve the coulombic efficiency of the cell.

Figure 7 shows the AC impedance spectra of the cells after 300 cycles. All of the spectra exhibit two overlapping semicircles due to different contributions. The first semicircle in the higher frequency range primarily arises from the resistance of the surface layer on the electrodes, and the second semicircle in the middle to low frequency range arises from the charge transfer resistance at the electrode-electrolyte interface.[25–27] The capacitance associated with the surface layer was much lower than a double layer capacitance related with the charge transfer process. The electrolyte resistance, estimated from the intercept on the real axis in the high-frequency range, decreased with the addition of $SiO_2(Li^+)$ and showed the lowest value at 4.0 wt% $SiO_2(Li^+)$. Total interfacial resistance, i.e., the sum of two different contributes, decreased with increasing content of $SiO_2(Li^+)$ particles, reaching a minimum at 4.0 wt% $SiO_2(Li^+)$. This result is consistent with previous research showing that the addition of a proper amount of inorganic filler is effective in decreasing the electrode interfacial resistance.[28,29] As mentioned previously, the presence of the hydrophilic poly(lithium acrylate) in the shell of the $SiO_2(Li^+)$

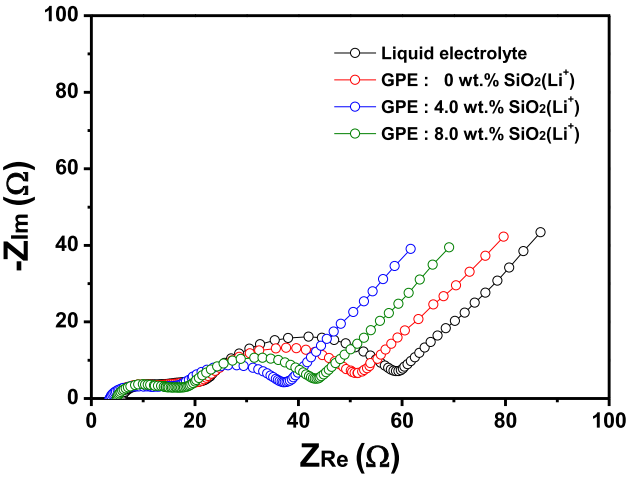

Figure 7. AC impedance spectra of lithium-ion polymer cells assembled with different electrolytes, which were measured after 300 cycles.

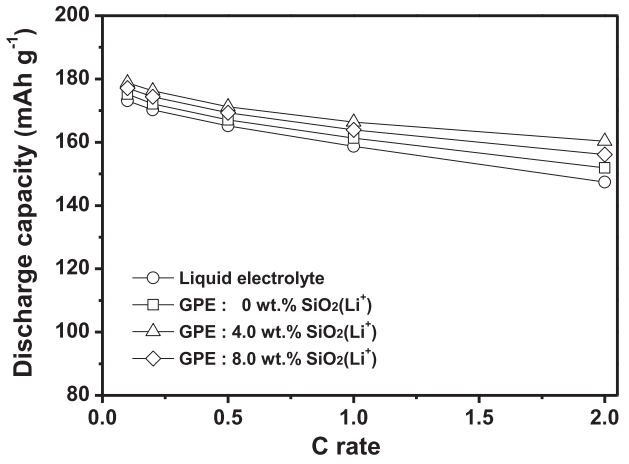

Figure 8. Discharge capacities of the lithium-ion polymer cells assembled with different electrolytes, as a function of the C rate.

particles was able to effectively hold the organic solvent. Thus, the harmful reactions between the organic solvent and the electrodes could be suppressed, which ultimately limited the growth of the resistive layer on the surfaces of the electrodes and resulted in an enhancement of interfacial stability. Poly(lithium acrylate) was also able to assist in adhering the composite polymer electrolyte to the electrodes, which gave favorable interfacial charge transport between the electrodes and the composite polymer electrolyte during cycling in the cell.

To evaluate the rate capability of the lithium-ion polymer cells, the cells were charged to 4.3 V at a constant current of 0.1 C and discharged at rates ranging from 0.1 to 2.0 C. Figure 8 shows that the content of $SiO_2(Li^+)$ particles affects the rate capability. The best performance was delivered by a cell assembled with composite polymer electrolyte containing 4.0 wt% $SiO_2(Li^+)$ particles. These results can be ascribed to efficient ionic conduction in the composite polymer electrolyte and favorable interfacial charge transport between the electrodes and the electrolyte in the cell containing 4.0 wt% $SiO_2(Li^+)$ particles. Note that the high rate performance of the cell with composite polymer electrolyte was much better than that of the cell with liquid electrolyte.

Figure 9a shows the charge-discharge curves of the lithium-ion polymer cell assembled with the composite polymer electrolyte containing 4.0 wt% $SiO_2(Li^+)$ particles at 55°C. The cell delivered an initial discharge capacity of 183.8 mAh g^{-1}, which is higher than that obtained at 25°C. When comparing the cycling stability of the cells at 55°C in Fig. 9b, the cell assembled with the composite polymer electrolyte containing 8.0 wt% $SiO_2(Li^+)$ particles exhibited the best capacity retention after 300 cycles (76.2%).

It is well known that the gradual capacity fading of layered $LiNi_xCo_yMn_{1-x-y}O_2$ materials at high temperatures is due to the dissolution of transition metals from the active cathode material by HF attack.[30,31] It is thus plausible that the cycling stability of the cell at high temperature is closely related to the content of HF in the composite polymer electrolytes. HF content in the different electrolytes was measured after storing the cells at 55°C for 3 days, and the results are shown in Fig. 10. HF content in the polymer electrolyte decreased with increasing content of $SiO_2(Li^+)$ particles. The oxygen atoms on poly(lithium acrylate) in the shell of the $SiO_2(Li^+)$ particles can complex with the reactive PF_5, which prevents PF_5 from being hydrolyzed to produce HF. Accordingly, the use of a composite polymer electrolyte with a high $SiO_2(Li^+)$ particle content inhibited the dissolution of transition metals from the active $LiNi_{0.6}Co_{0.2}Mn_{0.2}O_2$ material at elevated temperatures. As a result, the cell with 8.0 wt% $SiO_2(Li^+)$ particles exhibits the most stable cycling behavior at 55°C. In the case of a cell with liquid electrolyte, the dissolution of transition metals by HF attack may cause a rapid increase in the interfacial resistance, thereby accelerating the capacity loss as cycling progresses.

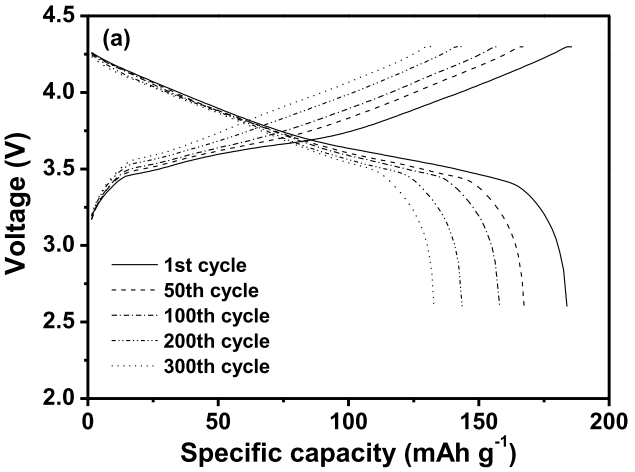

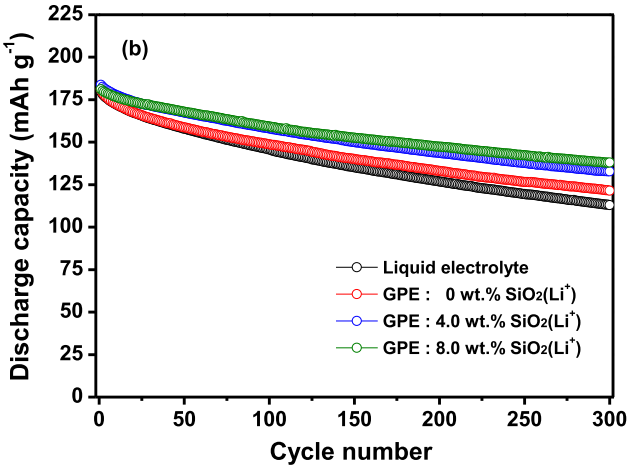

Figure 9. (a) Charge and discharge curves of the lithium-ion polymer cell assembled with composite polymer electrolyte containing 4 wt% $SiO_2(Li^+)$ nanoparticles at 55°C (0.5C CC and CV charge, 0.5C CC discharge, cut-off : 2.6–4.3 V) and (b) discharge capacities of the lithium-ion polymer cells assembled with different electrolytes at 55°C.

Conclusions

Core-shell-structured SiO_2 nanoparticles with poly(lithium acrylate) in their shell were synthesized and used in preparing Li^+

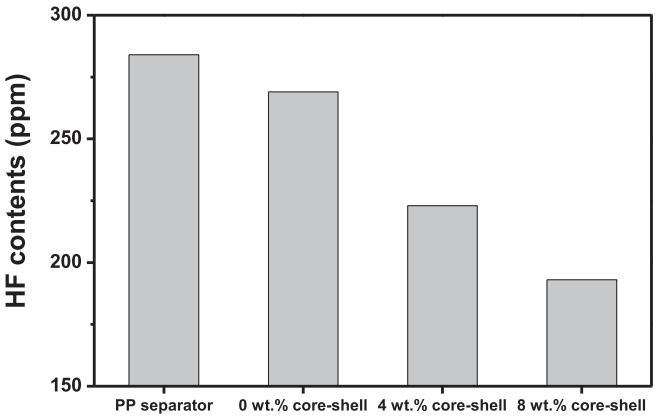

Figure 10. HF contents in the composite polymer electrolytes containing different contents of $SiO_2(Li^+)$ nanoparticles after being stored in 55°C oven for 3 days.

ion-conducting composite polymer electrolytes. The composite polymer electrolytes with $SiO_2(Li^+)$ particles exhibited high ionic conductivity, good wettability for electrolyte solution, good thermal stability, and favorable interfacial characteristics. The lithium-ion polymer cells assembled with composite polymer electrolyte containing a proper amount of $SiO_2(Li^+)$ particles were characterized by high discharge capacity, good high rate performance, and good cycling stability.

Acknowledgments

This work was supported by a National Research Foundation of Korea Grant funded by the Korean government (MEST) (NRF-2009-C1AAA001-0093307) and by a grant of the Human Resources Development Program of KETEP, funded by the Ministry of Trade, Industry and Energy of Korea (No. 20124010203290).

References

1. J. Hassoun, P. Reale, and B. Scrosati, *J. Mater. Chem.*, **17**, 3668 (2007).
2. J. W. Fergus, *J. Power Sources*, **195**, 4554 (2010).
3. E. Quartarone and P. Mustarelli, *Chem. Soc. Rev.*, **40**, 2525 (2011).
4. N. S. Choi, Z. Chen, S. A. Freunberger, X. Ji, Y. K. Sun, K. Amine, G. Yushin, L. F. Nazar, J. Cho, and P. G. Bruce, *Angew. Chem. Int. Ed.*, **51**, 9994 (2012).
5. J. Fan and P. S. Fedkiw, *J. Electrochem. Soc.*, **144**, 399 (1997).
6. D. W. Kim and Y. K. Sun, *J. Electrochem. Soc.*, **145**, 1958 (1998).
7. F. Croce, G. B. Appetecchi, L. Persi, and B. Scrosati, *Nature*, **394**, 456 (1998).
8. D. E. Strauss, D. Golodnitsky, and E. Peled, *Electrochem. Solid State Lett.*, **2**, 115 (1999).
9. N. Byrne, J. Efthimiadis, D. R. MacFarlane, and M. Forsyth, *J. Mater. Chem.*, **14**, 127 (2004).
10. H. Han, W. Liu, J. Zhang, and X.-Z. Zhao, *Adv. Funct. Mater.*, **15**, 1940 (2005).
11. A. S. Arico, P. Bruce, B. Scrosati, J.-M. Tarascon, and W. Van Schalkwijk, *Nat. Mater.*, **4**, 366 (2005).
12. Y. Aihara, G. B. Appetecchi, and B. Scrosati, *J. Electrochem. Soc.*, **149**, A849 (2002).
13. S. K. Das, S. S. Mandal, and A. J. Bhattacharyya, *Energy Environ. Sci.*, **4**, 1391 (2011).
14. C. Tang, K. Hackenberg, Q. Fu, P. M. Ajayan, and H. Ardebili, *Nano Lett.*, **12**, 1152 (2012).
15. Y. S. Lee, S. H. Ju, J. H. Kim, S. S. Hwang, J. M. Choi, Y. K. Sun, H. Kim, B. Scrosati, and D. W. Kim, *Electrochem. Commun.*, **17**, 18 (2012).
16. Y. S. Lee, J. H. Lee, J. A. Choi, W. Y. Yoon, and D. W. Kim, *Adv. Funct. Mater.*, **23**, 1019 (2013).
17. S. H. Ju, Y. S. Lee, Y. K. Sun, and D. W. Kim, *J. Mater. Chem. A*, **1**, 395 (2013).
18. W. K. Shin and D. W. Kim, *J. Power Sources*, **226**, 54 (2013).
19. Y. K. Sun, K. J. Hong, J. Prakash, and K. Amine, *Electrochem. Commun.*, **4**, 344 (2002).
20. J. P. Blitz, R. S. S. Murthy, and D. E. Leyden, *J. Colloid Interface Sci.*, **121**, 63 (1988).
21. P. Siberzan, L. Leger, D. Ausserre, and J. J. Benatta, *Langmuir*, **7**, 1647 (1991).
22. C. P. Tripp and M. L. Hair, *Langmuir*, **8**, 1120 (1992).
23. S. H. Goh, S. Y. Lee, X. Luo, and C. H. A. Huan, *Polymer*, **41**, 211 (2000).
24. M. C. Borghini, M. Mastragostino, S. Passerini, and B. Scrosati, *J. Electrochem. Soc.*, **142**, 2118 (1995).
25. A. Funabiki, M. Inaba, and Z. Ogumi, *J. Power Sources*, **68**, 227 (1997).
26. M. D. Levi, G. Salitra, B. Markovsky, H. Teller, D. Aurbach, U. Heider, and L. Heider, *J. Electrochem. Soc.*, **146**, 1279 (1999).
27. T. Liu, A. Garsuch, F. Chesneau, and B. L. Lucht, *J. Power Sources*, **269**, 920 (2014).
28. C. M. Yang, H. S. Kim, B. K. Na, K. S. Kum, and B. W. Cho, *J. Power Sources*, **156**, 574 (2006).
29. S. J. Lim, Y. S. Kang, and D. W. Kim, *Electrochim. Acta*, **56**, 2031 (2011).
30. G. G. Amatucci, J. M. Tarascon, and L. C. Klein, *Solid State Ionics*, **83**, 167 (1996).
31. S. U. Woo, B. C. Park, C. S. Yoon, S. T. Myung, J. Prakash, and Y. K. Sun, *J. Electrochem. Soc.*, **154**, A649 (2007).